Identification of Adult Mouse Neurovirulence Determinants of the Sindbis Virus Strain AR86

Mehul S. Suthar,[1] Reed Shabman,[1] Kenya Madric,[1] Cassandra Lambeth,[1] and Mark T. Heise[1,2]*

Department of Genetics[2] and Department of Microbiology and Immunology,[1] The University of North Carolina at Chapel Hill, Chapel Hill, North Carolina

Sindbis virus infection of mice has provided valuable insight into viral and host factors that contribute to virus-induced neurologic disease. In an effort to further define the viral genetic elements that contribute to adult mouse neurovirulence, the neurovirulent Sindbis virus strain AR86 was compared to the closely related (22 single amino acid coding changes and the presence or absence of an 18-amino-acid sequence in nsP3 [positions 386 to 403]) but avirulent Girdwood strain. Initial studies using chimeric viruses demonstrated that genetic elements within the nonstructural and structural coding regions contributed to AR86 neurovirulence. Detailed mapping studies identified three major determinants in the nonstructural region, at nsP1 538 (Ile to Thr; avirulent to virulent), an 18-amino-acid deletion in nsP3 (positions 386 to 403), and nsP3 537 (opal to Cys; avirulent to virulent), as well as a single determinant in the structural genes at E2 243 (Leu to Ser; avirulent to virulent), which were essential for AR86 adult mouse neurovirulence. Replacing these codons in AR86 with those found in Girdwood resulted in the attenuation of AR86, while the four corresponding AR86 changes in the Girdwood genetic background increased virulence to the level of wild-type AR86. The attenuating mutations did not adversely affect viral replication in vitro, and the attenuated viruses established infection in the brain and spinal cord as efficiently as the virulent viruses. However, the virus containing the four virulence determinants grew to higher levels in the spinal cord at late times postinfection, suggesting that the virus containing the four attenuating determinants either failed to spread or was cleared more efficiently than the wild-type virus.

The infection of mice with Sindbis-group viruses provides an excellent model for studying virus-induced neurologic disease. The outcome of Sindbis virus infection in the mouse model has been found to correlate with the age and strain of the animal, virus dose, route of inoculation, and virus strain (5, 6, 13, 31). The infection of neonatal mice with Sindbis virus results in a lethal disease characterized by elevated levels of proinflammatory cytokines and high viral titers in the muscles, brain, and serum in the absence of overt encephalitis (11, 26, 27). Increasing the age of the animal or infecting with an attenuated mutant virus results in a shift from systemic disease toward a neurologic disease; however, most Sindbis-group viruses are avirulent in mice greater than 14 days of age (28).

Previous neurovirulence studies with Sindbis-group viruses have identified virulence determinants in both the E2 glycoprotein gene (29, 30) and the 5′ noncoding region (3, 12). Studies with the neuroadapted Sindbis virus (NSV) identified a His at amino acid position 55 in the E2 glycoprotein that plays a major role in adult mouse neurovirulence (8, 30). The mechanism underlying this change is not yet completely understood; however, E2 His 55 was shown to correlate with improved binding and entry into neuronal cells (30), increased levels of viral replication (2), and the ability to overcome the protective effect of *bcl-2* overexpression in neurons (15, 16). Additionally,

a single substitution of a G at position 8 in the 5′ noncoding region of NSV was responsible for conferring neurovirulence in adult rats (12).

In addition to demonstrating the role of the structural genes in adult mouse neurovirulence, studies with the Sindbis virus S.A.AR86 (AR86) and Semliki Forest virus (SFV) indicate that the viral nonstructural genes contribute to adult mouse neurovirulence (9, 32, 33). Studies with AR86 have shown that the presence of a Thr at position 538 in nsP1 plays an important role in contributing to adult mouse neurovirulence. Replacing this Thr of AR86 with an Ile, found in most Sindbis-group viruses, attenuates the virus, while introduction of the Thr into a nonneurovirulent laboratory strain of Sindbis virus led to an increase in neurovirulence (9). The introduction of the attenuating Ile at position 538 in nsP1 did not affect viral growth, as viruses that contained this change replicated as well as wild-type AR86 both in cell culture and in the brains of infected animals. Furthermore, the presence of an Ile at position 538 accelerated processing of the nonstructural protein precursor (P123) into the mature nonstructural proteins, leading to earlier induction of viral 26S RNA synthesis during infection (10). In the case of SFV, mapping studies performed using virulent and avirulent strains demonstrated the importance of the nsP3 gene, including replacement of the opal termination codon (located within nsP3) with a sense codon, in reconstituting adult mouse neurovirulence (32, 33).

In this study, we utilized a newly generated clone of the Sindbis virus Girdwood to map determinants of adult mouse neurovirulence within AR86. While AR86 causes a lethal dis-

* Corresponding author. Mailing address: The Carolina Vaccine Institute, The University of North Carolina at Chapel Hill, 827 Mary Ellen Jones Building, CB #7292, Chapel Hill, NC 27599. Phone: (919) 966-1492. Fax: (919) 843-6924. E-mail: heisem@med.unc.edu.
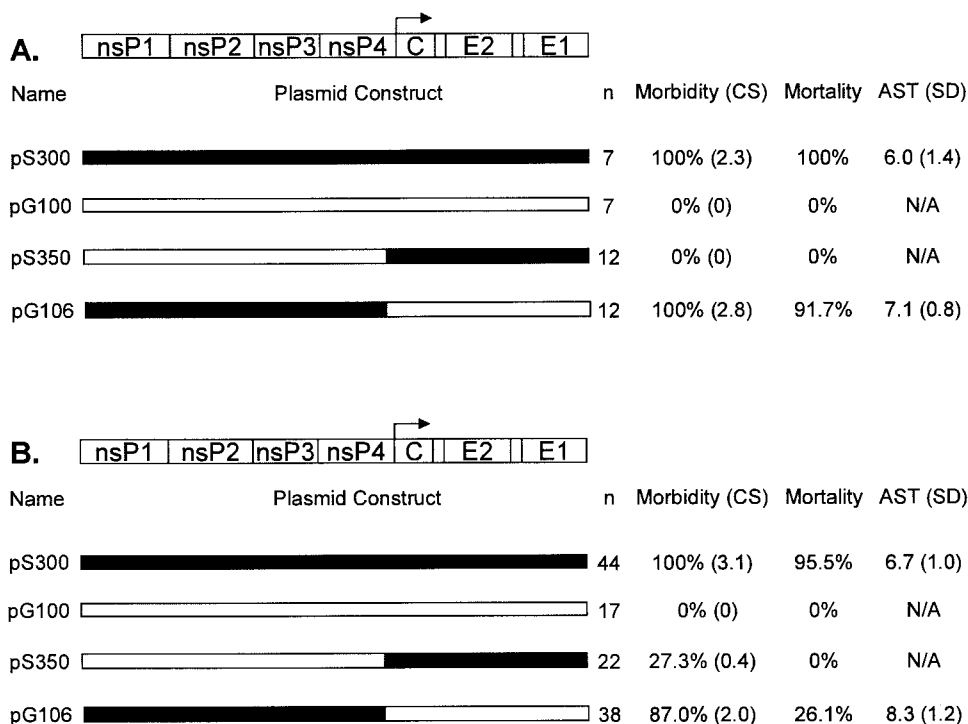
A. nsP1 | nsP2 | nsP3 | nsP4 | C | E2 | E1

Name	Plasmid Construct	n	Morbidity (CS)	Mortality	AST (SD)
pS300		7	100% (2.3)	100%	6.0 (1.4)
pG100		7	0% (0)	0%	N/A
pS350		12	0% (0)	0%	N/A
pG106		12	100% (2.8)	91.7%	7.1 (0.8)

B. nsP1 | nsP2 | nsP3 | nsP4 | C | E2 | E1

Name	Plasmid Construct	n	Morbidity (CS)	Mortality	AST (SD)
pS300		44	100% (3.1)	95.5%	6.7 (1.0)
pG100		17	0% (0)	0%	N/A
pS350		22	27.3% (0.4)	0%	N/A
pG106		38	87.0% (2.0)	26.1%	8.3 (1.2)

FIG. 1. Both the nonstructural and structural genes of AR86 contain neurovirulence determinants. A diagram of the *Alphavirus* genome organization is located at the top. On the left are the names of the cDNAs encoding full-length virus, beginning with the parental strains pS300 (wild-type AR86) and pG100 (wild-type Girdwood) and followed by the chimeric viruses. The cDNA constructs are diagrammed to show the sequences derived from pS300 (shaded box) and pG100 (open box). The chimeric clone pS350 contains AR86 nucleotide sequences between 1 and 6411, and the chimeric pG106 clone contains AR86 nucleotide sequences from 6411 to 11343. Groups (*n*, number of mice per group) of either 4-week-old (A) or 6-week-old (B) female CD-1 mice were inoculated i.c. with 10^3 PFU of each virus and observed daily for clinical signs. Virulence was assessed by morbidity (average clinical score [CS] on day 5), mortality, and average survival time (AST; number of days ± standard deviation [SD]).

ease in adult mice, Girdwood is avirulent, even when administered intracranially (i.c.). However, these viruses differ by only 22 single amino acid coding changes, as well as an 18-amino-acid sequence in nsP3 that is present in Girdwood but deleted from AR86. Detailed mapping studies localized determinants to both the nonstructural and structural genes. Furthermore, the virus containing the attenuating mutations did not adversely affect in vitro viral replication, and the attenuated viruses established infection in the brain and spinal cord as efficiently as the virulent viruses. However, at late times postinfection, the virus containing the virulence determinants grew to higher levels in the spinal cord, suggesting that the viruses containing the attenuating determinants either fail to spread or are cleared more efficiently than the virulent virus.

MATERIALS AND METHODS

Virus stocks and cell culture. Plasmids containing the viral cDNA are designated by the prefix "p," while the infectious virus derived from the cDNA clone does not contain the "p" designation; i.e., S300 represents virus derived from the plasmid pS300. Clone pS300 was derived from AR86 RNA, and S300 is comparable to AR86 virus both in its growth and in its virulence properties (23). Clone pS300 is identical to clone pS55 (23) except for a PmeI restriction site engineered at the 3' end of the viral 3' untranslated region (UTR) to facilitate generating chimeras with the Girdwood clone. Virus derived from the Girdwood cDNA clone also exhibits in vitro and in vivo phenotypes similar to the those of the Girdwood natural isolate (M. Suthar, unpublished data).

Virus stocks were made as described previously (9). Briefly, viral cDNA plasmids were linearized with PmeI and used as templates for the synthesis of full-length transcripts by using SP6-specific mMessage Machine in vitro tran-

scription kits (Ambion). Transcripts were electroporated into BHK-21 cells grown in α-minimal essential medium (10% fetal calf serum [Gibco], 10% tryptose phosphate broth σ, and 0.29 mg of L-glutamine [Gibco] per ml). Supernatants were harvested 24 to 27 h after electroporation, subjected to centrifugation at 3,000 rpm (Sorvall rotor RTH-250) for 20 min at 4°C, and frozen in 1-ml aliquots. Virus stocks were titrated on BHK-21 cells as previously described (23).

BHK-21 cells were maintained at 37°C in α-minimal essential medium for a maximum of 10 passages. Single-step in vitro growth curves were performed as previously described (9). Briefly, BHK-21 cells were plated at 10^5 cells/well in 24-well plates (Sarstedt) for 18 h at 37°C. Medium was removed, and wells were infected with virus in triplicate at a multiplicity of infection of 5.0. Cells were incubated at 37°C for 1 h. Wells were then washed three times with 1 ml of room-temperature phosphate-buffered saline (PBS) supplemented with 1% donor calf serum and Ca^{2+}-Mg^{2+}. One milliliter of growth medium was then added to each well, and cells were incubated at 37°C. Samples of supernatant were removed at various time points, with an equal volume of fresh medium added to maintain a constant volume within each well. Samples were frozen at −80°C until analysis by plaque assay.

Construction of full-length cDNAs and chimeric viruses. Standard recombinant DNA techniques were used to construct cDNA clones as previously described (21). The chimeric cDNA clone pS350, carrying the nsP1, nsP2, and nsP3 genes of Girdwood in the AR86 genome, was constructed by replacing the MfeI (nucleotide [nt] 43)-to-BstBI (nt 6411) fragment of pS300 with that of pG100 (Fig. 1). The chimeric cDNA clone pG106, carrying the structural genes of Girdwood in the AR86 genome, was constructed by exchanging the MfeI (nt 43)-to-BstBI (nt 6411) fragment of pG100 with that of pS300 (Fig. 1).

Clone pS341 (with changes of Ile to Val at position 648 and Leu to Glu at position 651 in nsP2), clone pS342 (with a Gly-to-Glu change at nsP3 position 344), and clone pS344 (with a Cys-to-opal termination codon change at nsP3 position 537) were created by PCR-mediated site-directed mutagenesis on the wild-type pS300 background (Fig. 2). Clone pS343, containing the Girdwood 18-amino-acid region in nsP3 between positions 386 and 403, was constructed by replacing the SfiI (nt 5122)-to-AatII (nt 5285) fragment of pS300 with that of
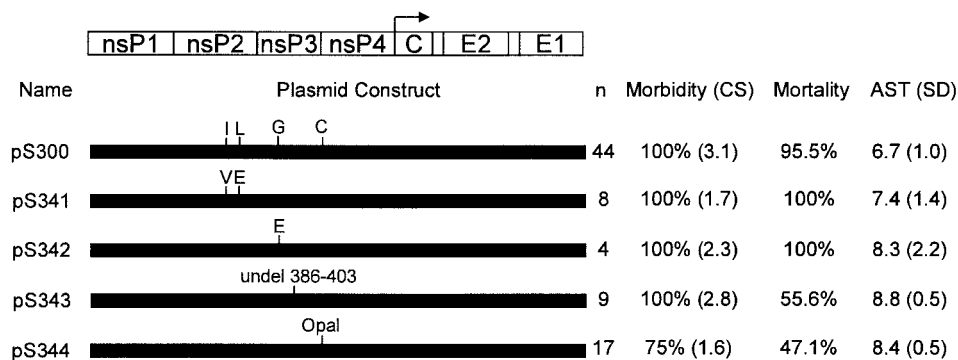
FIG. 2. Mutational analysis of neurovirulence determinants within the nonstructural genes of AR86. The cDNA constructs are diagrammed to show sequences derived from AR86 (pS300) along with amino acids located in nsP2 at positions 648 and 651 and nsP3 positions 344, 386 to 403, and 537. Groups (*n*) of 6-week-old female CD-1 mice were inoculated i.c. with 10^3 PFU of either wild-type AR86 (S300) or each mutant virus and observed daily for clinical signs. Virulence was assessed by morbidity (average CS on day 5), mortality, and AST (number of days ± SD). The mortalities for the mutant viruses S343 and S344 were statistically significant when compared to S300 (*P* < 0.05).

pG100. However, the introduction of this region also included a single amino acid change of a Glu at nsP3 position 344, which was subsequently corrected to a Gly by primer-directed mutagenesis.

For the following panel of nonstructural chimeric cDNA clones, AR86 genomic fragments or point mutations were introduced into the chimeric virus pS350 (Fig. 3). Clone pS351 was derived by replacing the thymidine with cytidine at nucleotide position 1672 using PCR megaprimer mutagenesis (22), which replaced an Ile with a Thr codon at nsP1 position 538. Clone pS352 was made by replacing the adenine with a thymidine at nucleotide position 5793 to replace the opal termination codon at nsP3 position 537 with a Cys codon. Clone pS353 was constructed by deleting the sequences between nucleotide positions 5257 and 5311, corresponding to amino acid positions 386 to 403 of nsP3 in Girdwood, by primer-directed mutagenesis. Clones pS354, pS355, pS356, and pS364, which contain different combinations of the changes at nsP1 position 538, nsP3 positions 386 to 403, and nsP3 position 537, were constructed by exchanging restriction fragments from clones pS351, pS352, and pS353.

For the panel of structural gene chimeric viruses listed in Fig. 4, AR86 genomic fragments or point mutations were introduced into the chimeric virus pG106. The StuI-BssHII fragment (nt 8110 to 9766), including most of the E2 coding region from clone pS300, was introduced into clone pG106 to create the chimeric clone pG107, and the BssHII-PmeI fragment (nt 9766 to 11343), encompassing most of the E1 coding region of clone pS300, was introduced into clone pG106 to create chimeric clone pG108. Clone pG117 was constructed by replacing the thymidine at position 9319 of pG106 with cytidine by PCR megaprimer mutagenesis, resulting in a coding change from a Ser to a Leu at E2 position 243. Chimeric clone pG163 was constructed by primer-directed mutagenesis of pG100 as follows: substitution of thymidine for cytidine at nucleotide 1672 (Ile to Thr at nsP1 538), deletion of nucleotides between 5257 and 5311 (18-amino-acid deletion from nsP3 386 to 403), substitution of adenine for thymidine at nucleotide 5765 (opal to Cys at nsP3 537), and substitution of thymidine for cytidine at nucleotide 9319 (Leu to Ser at E2 243). The reciprocal set of changes was made in pS300 to create clone pS363. Introduction of the various mutations was confirmed by sequencing at the
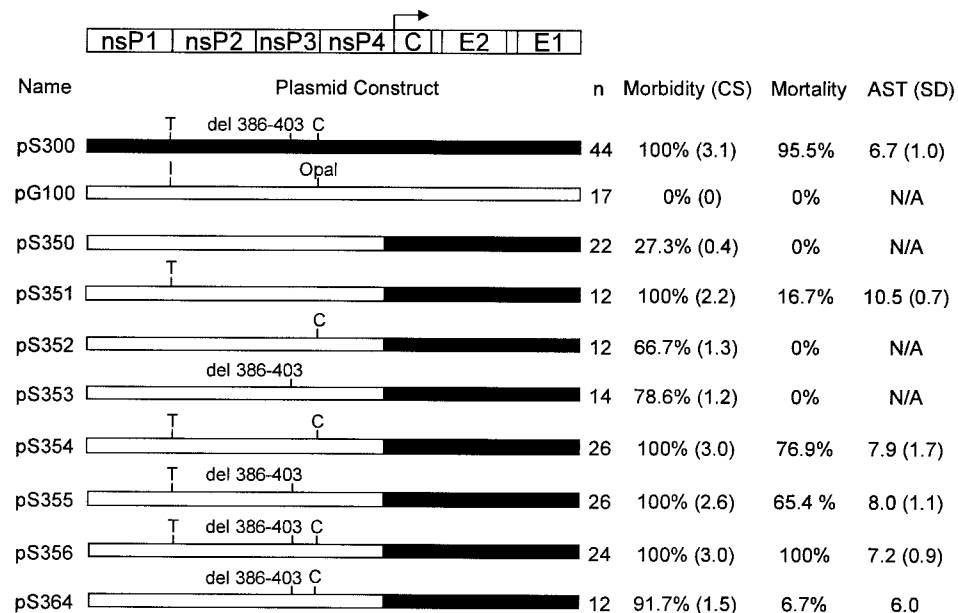

FIG. 3. AR86 neurovirulence determinants within the nonstructural genes. The cDNA constructs are diagrammed to show the sequences derived from pS300 (shaded box) and pG100 (open box) along with amino acids located in nsP1 at position 538 (Thr in pS300 and Ile in pG100), nsP3 between positions 386 and 403 (del 386-403 in pS300), and nsP3 at position 537 (Cys in pS300 and Opal in pG100). All of the chimeric clones contain AR86 nucleotide sequences between 6411 and 11343. Groups (*n*) of 6-week-old female CD-1 mice were inoculated i.c. with 10^3 PFU of each virus and observed daily for clinical signs. Virulence was measured by morbidity (average CS on day 5), mortality, and AST (average number of days ± SD). The mortalities for the chimeric viruses S354, S355, and S356 were statistically significant when compared to the parental chimeric virus S350 (*P* < 0.05).
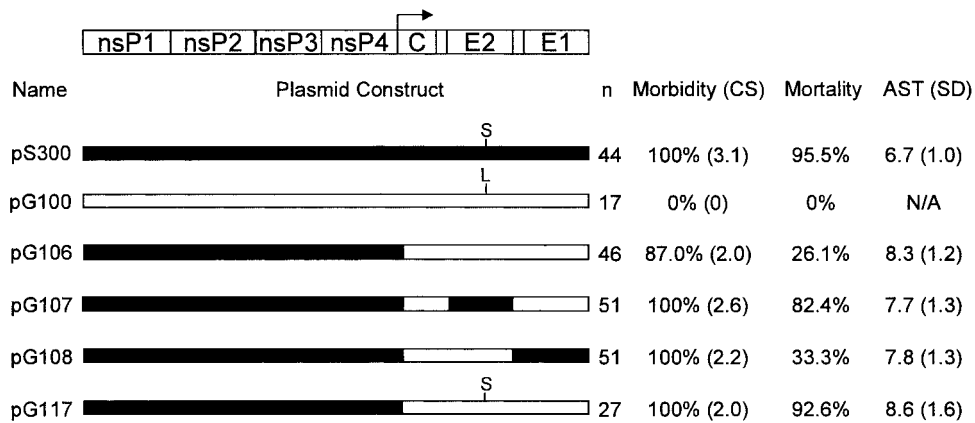
FIG. 4. AR86 neurovirulence determinants within the structural genes. The cDNA constructs are diagrammed to show the sequences derived from pS300 (shaded box) and pG100 (open box) along with the amino acid located in E2 at position 243 (Ser in pS300 and Leu in pG100). All of the chimeric clones contain AR86 nucleotide sequences between 1 and 6411. Groups (*n*) of 6-week-old female CD-1 mice were inoculated i.c. with 10^3 PFU of virus and observed daily for clinical signs. Virulence was assessed by morbidity (average CS on day 5), mortality, and AST (average number of days ± SD). The mortalities for the chimeric viruses G107 and G117 were statistically significant when compared to the parental chimeric virus G106 ($P < 0.05$).

University of North Carolina at Chapel Hill (UNC-CH) Genome Analysis Facility with a model 373A DNA sequencing apparatus (Applied Biosystems). Chimeric virus stocks derived from full-length cDNAs were made as described above.

Animal studies. Specific-pathogen-free female CD-1 mice were obtained from Charles River Breeding Laboratories (Raleigh, N.C.). Animal housing and care were in accordance with all UNC-CH Institutional Animal Care and Use Committee guidelines. Six-week-old mice were anesthetized with either isoflurane (Halocarbon Laboratories) or ketamine supplemented with xylazine (Barber Med.) prior to i.c. inoculation with a standard dose of 10^3 PFU of virus in diluent (PBS, pH 7.4) supplemented with 1% donor calf serum (Gibco). Mock-infected mice received diluent alone. Mice were monitored daily for body weight and scored for clinical signs as follows: (i), ruffled fur and/or hunched body posture; (ii), mild hind-limb dysfunction; (iii), prominent hind-limb dysfunction; (iv), severe hind-limb dysfunction; (v), paralysis of hind limbs; and (vi), terminal morbidity. The average clinical score was calculated on day 5. This day was chosen because by day 6 infected mice reproducibly showed severe disease progression and occasionally were euthanized, with death being recorded for the following day. As required by the UNC-CH animal protocol, infected mice were euthanized during the experiment either when mice dropped below 30% of initial body weight or when mice exhibited severe disease signs. Statistical analysis for mortality was performed using Fisher's exact chi-square test, and differences were considered significant when *P* was <0.05 (Instat 3.0). For the in vivo growth studies, mice were inoculated as described above and sacrificed by exsanguination followed by perfusion with 10 ml of PBS at 6, 12, 24, 48, 72, 96, and 120 h postinfection. The whole brain was removed and weighed, and viral load was assessed by plaque assay on BHK-21 cells (9, 23). The spinal cord was removed, divided into thoracic and lumbar regions, and weighed, and viral loads were evaluated by plaque assay on BHK-21 cells.

RESULTS

Neurovirulence determinants are localized within both nonstructural and structural genes of AR86. Sindbis virus adult mouse neurovirulence determinants have previously been found in the viral 5′ noncoding region UTR and the E2 glycoprotein (12, 29). In addition, previous studies with AR86 identified a single coding change at nsP1 position 538 that was essential for adult mouse neurovirulence (9). In an effort to identify additional virulence determinants within AR86, comparisons were made between AR86 and Girdwood virus, a Sindbis virus that is closely related to AR86 but nonneurovirulent in adult mice. To confirm neurovirulence phenotypes, mice were inoculated i.c. with 10^3 PFU of either S300 (AR86) or G100 (Girdwood) virus and monitored for virus-induced morbidity and mortality. Mice were observed daily and scored for clinical signs, such as

weight loss, ruffled fur, hunched body posture, hind-limb dysfunction (mild, moderate, and severe), paralysis of hind limbs, and terminal morbidity. The average clinical score (CS) for each group was calculated from observations made on day 5. Consistent with previous reports, S300 caused 100% morbidity and 100% mortality in 4-week-old mice, while G100 caused no detectable morbidity or mortality in the infected mice (Fig.

TABLE 1. Amino acid sequence comparison between AR86 and Girdwood

Gene	Amino acid position[a]	Amino acid in:	
		AR86	Girdwood
nsP1	469	Met	Ile
	537	Thr	Ile
nsP2	30	Ile	Thr
	187	Thr	Ala
	218	Glu	Gln
	295	His	Tyr
	485	Ala	Arg
	634	Glu	Lys
	648	Ile	Val
	651	Lys	Glu
nsP3	344	Gly	Glu
	346	Val	Ala
	386–403[b]	Deletion	
	386[c]	Tyr	Asp
	442	Asp	Gly
	446	Ile	Met
	537	Cys	opal
E2	243	Ser	Leu
6k	30	Val	Ile
E1	61	Arg	Lys
	112	Val	Ala
	169	Leu	Ser

[a] Amino acid numbering is from AR86.
[b] nsP3 18-amino-acid deletion found in AR86.
[c] First amino acid after 18-amino-acid deletion.

1A). G100 and S300 differ at 22 single amino acid positions and by the presence (G100) or absence (S300) of an 18-amino-acid sequence in nsP3 (Table 1). Given that the coding differences between S300 and G100 were distributed throughout the genome, our initial strategy involved defining whether the viral nonstructural or structural genes contained the major determinants of AR86 virulence. Therefore, two chimeras containing either the AR86 nonstructural genes with the G100 structural genes (G106) or the G100 nonstructural genes with the AR86 structural genes (S350) were constructed and evaluated for virulence following i.c. infection of 4-week-old CD-1 mice. G106 caused 91.7% mortality and 100% morbidity, while S350 caused neither morbidity nor mortality (Fig. 1A), though this virus grew as well as either wild-type parent (S300 or G100) both in vitro and in vivo (data not shown). Furthermore, in vitro transcripts of pS300, pG100, pS350, and pG106 exhibited similar specific infectivities (data not shown). These results strongly suggested that the major determinants of AR86 neurovirulence were located in the nonstructural coding region. However, when older mice (6 weeks old) were inoculated i.c. with G106, only 26.1% mortality was observed, in comparison to 95.5% mortality with S300 (Fig. 1B). Therefore, it was likely that determinants in both the nonstructural and structural genes were required for the full neurovirulence of AR86.

Since AR86 virulence determinants appeared to be located in both the structural and nonstructural genes, mapping of these virulence determinants was done separately, with the initial focus on the nonstructural region. While it was possible that noncoding differences were at least partly responsible for the virulence differences between AR86 and Girdwood, the initial analysis focused on the coding differences, which were located in nsP1, nsP2, and nsP3 but not nsP4 (Table 1). Previous analysis indicated that eight of the coding differences, as well as the nsP3 deletion, were unique to AR86 when it was compared to the known coding sequences of five nonvirulent Sindbis viruses (23). Furthermore, in previous studies, the unique Thr at nsP1 538 of AR86 was shown to be essential for adult mouse neurovirulence, as viruses with Ile at this position no longer caused lethal disease in adult mice (9). This result suggested that other coding changes that were unique to AR86 might be virulence determinants. Therefore, each of the AR86-specific coding changes, with the exception of two changes at codons 442 and 446 in nsP3, were changed in the S300 background to the codon found at the corresponding position in Girdwood (clones pS341 and pS342). The role of the 18-amino-acid deletion was also assessed by reintroducing the 18-amino-acid sequence found at nsP3 positions 386 to 403 of Girdwood and the other nonneurovirulent Sindbis viruses back into the S300 clone (clone pS343), and an opal codon was introduced at nsP3 position 537 (pS344). The specific changes introduced into each clone were confirmed by sequencing. Viruses derived from these clones were evaluated for a loss of virulence following i.c. inoculation of 10^3 PFU into 6-week-old CD-1 mice. In the process of performing this analysis, it became apparent that the reported Arg codon at position 256 of nsP2 in the AR86 infectious clone (23) was actually an Ala codon, which is present in all of the other Sindbis virus genomes. Therefore, this position was dropped from our analysis. Three changes at positions 648 and 651 of nsP2 (clone pS341) and at position 344 of nsP3 (clone pS342) did not appear to be

major contributors to the adult mouse neurovirulence phenotype of AR86, since changing these codons to the corresponding codon found in Girdwood did not affect virulence in S300 (Fig. 2). However, reintroduction of the 18-amino-acid deletion in nsP3 (clone pS343), or changing the unique Cys codon at nsP3 position 537 back to the opal termination codon (clone pS344) found in most nonneurovirulent Sindbis viruses altered S300 virulence (Fig. 2). In addition, both of these viruses exhibited growth kinetics equivalent to the wild-type S300 virus in vitro, suggesting that the decreased virulence was not simply due to a decrease in virus growth (data not shown). These results suggested that in addition to nsP1 position 538 (9), additional AR86 virulence determinants included the 18-amino-acid deletion in nsP3 and the Cys codon at nsP3 537, while the unique codons at nsP2 648 and 651 or nsP3 344 did not appear to contribute to adult mouse virulence. The role of nsP3 442 and 446 was not addressed in this analysis, but the contribution of these determinants to virulence was evaluated in later studies (see below).

Introduction of AR86 determinants into the nonvirulent Girdwood background results in a gain of virulence. Though the mutation of nsP3 537 (Cys to opal) or the reintroduction of the 18-amino-acid deletion into nsP3 on the S300 background resulted in a loss of virulence, it was possible that rather than being true virulence determinants, these changes simply decreased virus fitness and thereby caused a subtle decrease in virus replication which affected virulence. Therefore, a more rigorous test of whether these or other determinants within the nonstructural genes were virulence determinants was performed by introducing changes into the nonneurovirulent Girdwood background (clone pG100) and assaying for a gain of virulence. Since the AR86 nonstructural genes did not confer wild-type levels of virulence in the absence of the AR86 structural genes, all nonstructural mapping studies were performed using the clone pS350, which contained the Girdwood nonstructural region and the AR86 structural genes. Therefore, if all of the nonstructural determinants of virulence were introduced into the pS350 clone, the resulting virus should exhibit a level of neurovirulence comparable to that of AR86. As an initial step in this process, the three loci that were implicated in the S300 analysis (Fig. 2) (9) were analyzed in the S350 background by introducing the codon found in the virulent AR86 virus back into the corresponding position in the Girdwood nonstructural region and looking for a gain of virulence (Fig. 3).

The introduction of a Thr codon in place of the Ile at nsP1 538 in the nonneurovirulent Sindbis virus TR339 was previously shown to increase virulence in 18- to 21-day-old mice (9), which strongly suggests that this determinant plays a major role in adult mouse neurovirulence. When a Thr codon was placed at nsP1 538 of the pS350 clone, the resulting virus (S351) caused 100% morbidity, with a day 5 average clinical score of 2.2, and 16.7% mortality (Fig. 3), compared to 27.3% morbidity (with a day 5 average clinical score of 0.4) and 0% mortality with the S350 virus. A virus (S352) where the consensus opal termination codon at nsP3 position 537 was replaced with the AR86-derived Cys codon caused 66.7% morbidity (day 5 average clinical score of 1.3) but no mortality (Fig. 3). Likewise, deleting the 18 amino acids from positions 386 to 403 in nsP3 of clone S350 (virus designated S353) gave 78.6% morbidity
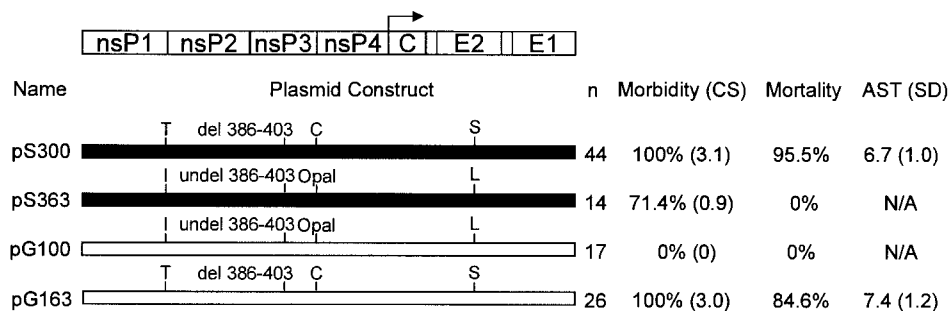
FIG. 5. Identification of the major determinants of neurovirulence within AR86. The cDNA constructs are diagrammed to show the sequences derived from pS300 (shaded box) and pG100 (open box) along with amino acids located in nsP1 at position 538 (Thr in pS300 and Ile in pG100), nsP3 between positions 386 and 403 (del 386-403 in pS300), nsP3 at position 537 (Cys in pS300 and Opal in pG100), and E2 at position 243 (Ser in pS300 and Leu in pG100). Groups (n) of 6-week-old female CD-1 mice were inoculated i.c. with 10³ PFU of virus and observed daily for clinical signs. Virulence was measured by morbidity (average CS on day 5), mortality, and AST (average number of days ± SD).

(day 5 average clinical score of 1.2) but no mortality (Fig. 3). Therefore, all three changes independently increased S350 virulence as determined by an increase in virus-induced morbidity; however, none of the individual determinants were able to raise S350 virulence to the level observed with AR86 (clone S300). Therefore, the individual coding changes were evaluated in combination. The introduction of both the 18-amino-acid deletion and the Cys codon at nsP3 position 537 of clone ps350 resulted in a virus (S364) that caused 91.7% morbidity (day 5 average clinical score of 1.5) and 6.7% mortality (Fig. 3). However, when the Thr at nsP1 position 538 was introduced into clone pS350 in combination with either the 18-amino-acid deletion (clone ps355) or the Cys codon at nsP3 position 537 (clone ps354), the resulting viruses were significantly more virulent than the parental S350 virus (27.3% morbidity and 0% mortality) (Fig. 3). The S355 virus (Thr at nsP1 538 and 18-amino-acid deletion at nsP3 386 to 403) caused 100% morbidity and 65.4% mortality in 6-week-old mice, while the S354 virus (Thr at nsP1 538 and Cys at nsP3 537) caused 100% morbidity and 76.9% mortality (Fig. 3). Finally, when all three changes were introduced into the same virus (clone pS356), the resulting virus caused 100% morbidity and 100% mortality in 6-week-old mice following i.c. inoculation. Therefore, the Thr at nsP1 position 538, the 18-amino-acid deletion from nsP3 386 to 403, and the Cys at nsP3 537 are the major determinants of AR86 neurovirulence within the AR86 nonstructural genes. Minor roles for other coding changes, such as nsP3 positions 442 and 446, or noncoding changes cannot be ruled out; however, they were not necessary for the full adult mouse neurovirulence phenotype in the Girdwood background.

Serine at position 243 in the E2 glycoprotein is a major determinant of AR86 adult mouse neurovirulence. Both the AR86 nonstructural genes determinants and the AR86 structural genes were required for complete neurovirulence (Fig. 1). Therefore, studies were initiated to identify the structural gene determinants that contributed to adult mouse virulence. Since complete virulence required the AR86 nonstructural genes, all structural gene mapping studies were conducted using the G106 clone, which contains the AR86 nonstructural genes and the Girdwood structural genes and causes 87.0% morbidity (day 5 average clinical score of 2.0) and 26.1% mortality. Gene segments or individual coding changes from the structural genes of wild-type AR86 (pS300) were introduced back into

pG106, and the resulting viruses were evaluated for increased virulence following i.c. inoculation of adult mice. The AR86 and Girdwood structural genes contained five coding differences: one difference in the E2 glycoprotein, one in the 6k protein, and three in the E1 glycoprotein. The relative contribution of the change in E2 versus the changes in the 6k and E1 protein coding regions were assessed by using two chimeras where the E2 coding region or the 6k and E1 coding region of AR86 was introduced into the G106 background. When these viruses were evaluated for virulence, the virus with the AR86 E2 gene (G107) caused 100% morbidity and 82.4% mortality (Fig. 4), while the virus with the AR86 6k and E1 coding region caused 100% morbidity (day 5 average clinical score of 2.2) and 33.3% mortality (Fig. 4). While these results suggest that minor determinants of AR86 neurovirulence reside within the 6k and E1 coding region, it is clear that a major determinant of adult mouse neurovirulence was located in the E2 glycoprotein. Since AR86 and Girdwood differ only at position 243 of E2, it was likely that this was the major determinant of adult mouse neurovirulence within the AR86 structural proteins. This possibility was directly tested by introducing the Ser codon at E2 position 243 into the G106 clone to create the virus G117. While G106 caused 87.0% morbidity (day 5 average clinical score of 2.0) and 26.1% mortality, clone G117 caused 100% morbidity (day 5 average clinical score of 2.0) and 92.6% mortality, suggesting that the Ser at E2 position 243 was a major determinant of adult mouse neurovirulence (Fig. 4). Although the average peak clinical scores for G106 and G117 are the same on day 5, G117-infected mice progress to show more severe disease and increased mortality.

Determinants at nsP1 538, nsP3 386 to 430, nsP3 537, and E2 243 are able to confer an adult mouse neurovirulence phenotype in the Girdwood genetic background. In order to determine whether the three nonstructural determinants and the Ser codon at E2 position 243 were the major determinants of adult mouse neurovirulence in the AR86 virus, the four determinants were introduced into the G100 background. While G100 caused no morbidity or mortality in 6-week-old mice, the virus G163, which was identical to G100 except for the presence of an Ile-to-Thr change at nsP1 538, an 18-amino-acid deletion from nsP3 positions 386 to 403, an opal-to-Cys change at nsP3 537, and a Leu-to-Ser change at E2 243, caused 100% morbidity (day 5 average clinical score of 3.0) and 84.6%
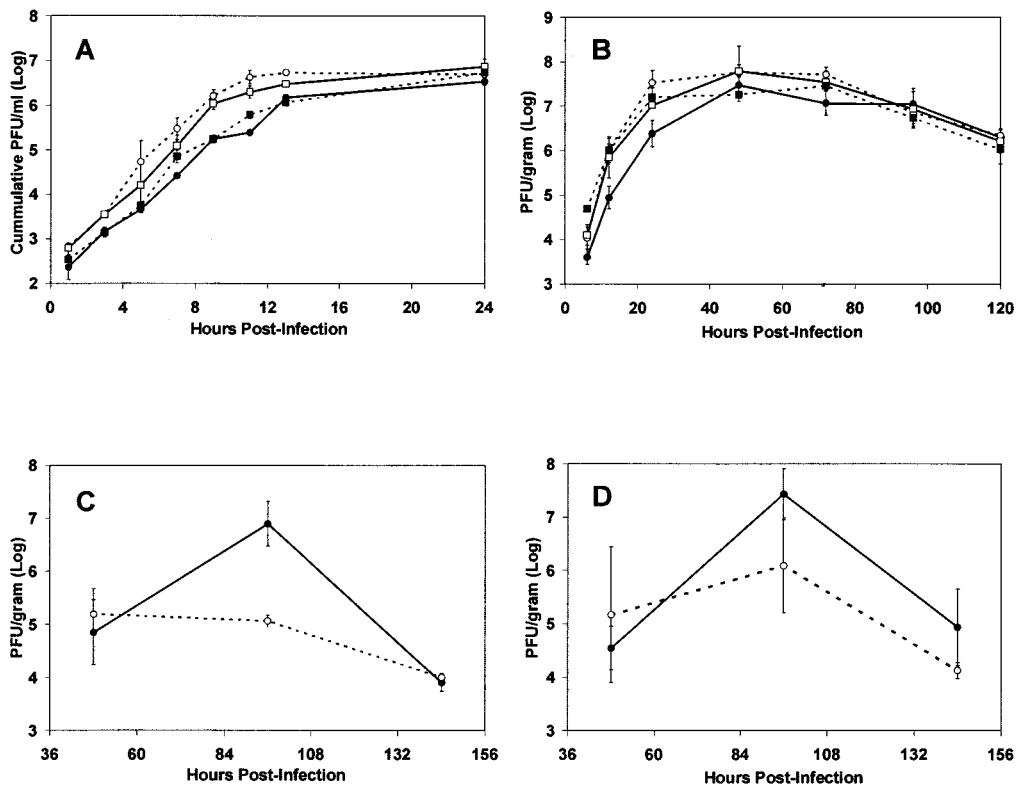
FIG. 6. In vitro and in vivo growth analysis of virulent and attenuated viruses. (A) A single-step in vitro growth curve was performed on BHK-21 cells infected with S300 (solid line, filled circle), S363 (broken line, open circle), G100 (solid line, open square), or G163 (broken line, filled square) at an MOI of 5.0. Shown are data from a representative experiment where each point represents the average of results from three independent samples ± SD. (B) Six-week-old female CD-1 mice were infected i.c. with 10^3 PFU of S300 (solid line, filled circle), S363 (broken line, open circle), G100 (solid line, open square), and G163 (broken line, filled square). Mice were sacrificed by exsanguination at 6, 12, 24, 48, 72, 96, and 120 h postinfection and perfused with PBS (pH 7.4). The brain was harvested and evaluated for viral load by plaque assay on BHK-21 cells. The data shown represent results from one of three experiments for the brain. (C and D) Six-week-old CD-1 mice were infected with S300 (solid line, filled circle) or S363 (broken line, open circle) as in panel B. Mice were sacrificed at 48, 96, or 144 h postinfection and perfused with PBS, and viral titers in the thoracic or lumbar spinal cord were determined by plaque assay. (C) Viral titers in the thoracic spinal cord ($n = 3$ mice per time point; data shown represent results from one of two identical experiments). (D) Viral loads in the lumbar spinal cord. Data were pooled from two experiments and six mice per time point. Differences in viral loads in the thoracic and lumbar spinal cord at 96 h postinfection are statistically significant ($P < 0.05$) as measured by two-tailed Student's t test.

mortality (Fig. 5). For comparison, the same four changes were introduced into the S300 background; however, in this case the changes were Thr to Ile at nsP1 538, reconstitution of nsP3 codons 386 to 403, Cys to opal at nsP3 537, and Ser to Leu at E2 243. This virus, which was designated S363, caused 71.4% morbidity (day 5 average clinical score of 0.9) and 0% mortality, in contrast to the parental S300 virus, which caused 100% morbidity (day 5 average clinical score of 3.1) and 95.5% mortality (Fig. 5). These results show that the introduction of the four AR86 determinants back into the nonvirulent Girdwood background resulted in a virus that exhibited neurovirulence that was comparable to AR86, demonstrating that these four changes play a major role in the adult mouse neurovirulence phenotype of AR86. However, minor contributions from other coding or noncoding differences between Girdwood and AR86 cannot be ruled out.

In vitro and in vivo growth analysis of the attenuated and virulent viruses. The differences in virulence between the attenuated viruses (G100 or S363 chimera) and the virulent viruses (S300 or G163 chimera) could simply be explained by replication efficiency or the ability to successfully establish in-

fection within neural tissues. Therefore, a single-step in vitro growth assay was performed for each virus in BHK-21 cells. As shown in Fig. 6A, the attenuated viruses grew at least as well as the virulent viruses at all time points tested. Viral growth in the brains and spinal cords of infected mice was evaluated next. Though G100 and S363 are significantly attenuated with regard to causing disease, both of these viruses grew at least as well as the virulent S300 and G163 viruses in the brains of infected mice at all times postinfection (Fig. 6B). Furthermore, when viral growth in the spinal cord was evaluated for S363 (attenuated) and S300 (virulent), viral titers were equivalent at 48 h postinfection, suggesting that both viruses were able to establish infection within the spinal cord. However, at 96 h postinfection, which is a time point when mice are starting to develop virus-induced disease signs, the virulent S300 virus exhibited significantly higher titers ($P < 0.05$) in the spinal cord than the attenuated S363 virus (Fig. 6C and D). This result suggests that the virus containing the four attenuating determinants is either defective in its ability to spread within the spinal cord or cleared more efficiently than the virus containing the four virulence determinants. Additional studies to evaluate the ex-

tent of viral replication within these tissues will be required to address this question.

DISCUSSION

The identification of the molecular determinants of alphavirus virulence represents an important step in understanding the pathogenesis of alphavirus-induced neurologic disease. The majority of studies looking at alphavirus neurovirulence determinants have identified the structural gene E2 and the 5′ noncoding region as major determinants of virulence in both neonatal and adult mice (3, 19, 29). However, recent work with the Sindbis virus AR86 and Semliki Forest virus has demonstrated a role for the nonstructural genes in mediating alphavirus neurovirulence (9, 32, 33). In this report, we describe the identification of four coding changes as major determinants of AR86 neurovirulence: at nsP1 position 538, at nsP3 position 537, an 18-amino-acid deletion from nsP3 386 to 403, and at E2 position 243. The fact that these four changes conferred adult mouse neurovirulence on a normally nonneurovirulent Sindbis virus argues that these changes represent the major determinants of AR86 neurovirulence, although contributions from additional AR86 determinants cannot be ruled out. It is also important to note that the neurovirulence determinants did not appear to simply affect viral replication in vitro or in neural tissue at early times postinfection (Fig. 6). However, studies in the spinal cord suggest that the attenuated viruses are either defective in spreading at late times in the infection or may be cleared more efficiently than the virulent viruses (Fig. 6). Additional work is required to assess these possibilities and also determine whether the differences between the virulent and attenuated viruses are spinal cord specific or whether there was a lack of sensitivity in detecting differences in the brain by plaque assay.

It is striking that all four of the identified AR86 neurovirulence determinants are, to our knowledge, unique to AR86 and not present in the published sequences of nonadult mouse-neurovirulent Sindbis viruses (23). Furthermore, these determinants do not appear to be shared with other adult mouse-neurovirulent Sindbis viruses, such as the NSV strain (3, 19, 31). This result suggests that AR86 and NSV have evolved different strategies for causing neurologic disease in adult mice. For instance, while the nonstructural gene determinants of AR86 are essential for neurovirulence in adult mice, the E2 243 change is only essential in mice greater than 4 weeks of age (Fig. 1). In contrast, the structural genes of the NSV strain of Sindbis are the major determinants of adult mouse neurovirulence, with a His at E2 position 55 being particularly important (31). There are several potential explanations for the differences in virulence determinants between AR86 and NSV, including passage histories and strain variation in the original viral isolates from which these neurovirulent viruses were derived. NSV was originally derived from the AR339 strain of Sindbis (7), while AR86 and Girdwood, which are closely related to each other, were isolated in South Africa. In fact, Girdwood is one of the few Sindbis viruses isolated from an infected human (20). Therefore, it is possible that genetic differences between the AR339 strain and the South African Sindbis virus strains, such as AR86 and Girdwood, biased these viruses toward different types of virulence determinants. NSV

and AR86 were also placed under different types of selective pressure during their early passages. NSV was derived from a virus that was passaged an unknown number of times in cell culture and then selected through six rounds of passage in neonatal and weanling mice (7). In contrast, AR86 was isolated from a mosquito pool and subjected to 45 to 60 alternating rounds of intracranial passage in neonatal and weanling mice (34), with very limited exposure to cell culture prior to the generation of the infectious clone (23). It is likely that these vastly different passage histories are in part responsible for the differences in virulence determinants between AR86 and NSV.

While all four changes are essential for the complete mouse neurovirulence phenotype of AR86, it appears that the Thr at nsP1 538 plays a particularly important role. Previous studies have shown that changing the Thr at nsP1 538 in AR86 to the consensus Ile found in nonneurovirulent viruses results in a complete loss of virus-induced mortality, though this virus was still capable of causing disease (9). Likewise, the introduction of a Thr codon at nsP1 position 538 into S350 (which contains the AR86 structural genes in the Girdwood virus background), creating S351, did not result in a complete restoration of neurovirulence, but a partial gain of virulence was observed (100% morbidity and 16.7% mortality [Fig. 3]). As for the mechanism underlying the role for nsP1 538 in virulence, we have previously reported that the substitution of the wild-type Thr with an Ile residue accelerates processing of the P123 polyprotein precursor into the mature nsP1, nsP2, and nsP3 proteins (10). This coincided with a more rapid induction of 26S RNA synthesis, contributing to earlier expression from the 26S promoter in infected cells, but did not measurably affect the levels of viral minus- or plus-strand RNA synthesis (10). The role of altered nonstructural polyprotein processing and/or accelerated induction of 26S RNA synthesis in adult mouse neurovirulence has yet to be determined. They may be acting through one or more mechanisms, including induction of immune mediators by the earlier 26S RNA expression, enhanced cytopathic effect due to high-level expression of the viral structural genes, or differential effects on host macromolecular synthesis due to differences in the ratios of the nonstructural polyprotein precursor to mature nonstructural proteins.

The 18-amino-acid deletion between residues 386 and 403 in nsP3 is located within the C-terminal region, which is highly variable between alphaviruses (as reviewed in reference 25). The function for the nsP3 protein has yet to be defined. However, it has been shown to be a phosphoprotein that is required for the synthesis of both viral minus-strand and subgenomic RNA (14, 17). It is interesting that the 18-amino-acid deletion results in the removal of 7 Ser residues, which may affect the overall phosphorylation of nsP3. Mutational analysis within the nonconserved C-terminal region of Sindbis virus nsP3 altered levels of viral minus-strand RNA synthesis, along with levels of nsP3 phosphorylation (14). Therefore, it will be important to assess the effect of the 18-amino-acid deletion on viral minus-strand synthesis. Recently, it was reported that mutations within the nsP3 gene of SFV, including a 7-amino-acid deletion within the C-terminal region, fully restored neurovirulence in adult mice (32), which suggests that nsP3 may contribute to the virulence of multiple alphaviruses. However, more analysis is required to determine the exact role for the AR86 nsP3 in adult mouse neurovirulence.

While most alphaviruses carry an opal termination codon proximal to the 3′ end of the nsP3 gene, the Sindbis virus strain AR86 (23) and the SFV strain SFV4 carry a sense codon, which has been shown to be an important contributor to neurovirulence in adult mice (23, 32, 33). Tuittila and Hinkkanen performed a detailed mapping study within the replicase genes using virulent and avirulent SFV strains and found that an Arg (virulent SFV4 strain) at nsP3 position 469, in place of the opal termination codon, was an important contributor to the adult mouse neurovirulence phenotype (32). The mechanism of this change in pathogenesis is not well understood. Translational readthrough of the opal termination codon occurs at a frequency of about 5 to 10% (as reviewed in reference 4), leading to limiting quantities of the nsP4 protein relative to the other nonstructural proteins. Interestingly, the nsP4 protein was found to be tightly regulated within infected cells, in that excess nsP4 was shown to be rapidly degraded by the N-end rule pathway (1). It is also worth noting that a different nsP3 C terminus is produced in viruses carrying either an opal termination codon or a sense codon. In the presence of an opal termination codon, the predominate nsP3 C terminus is produced by the translational stop codon, while in the presence of a sense codon, an extra 7 amino acids are added to the C terminus of nsP3. It is well known that the opal termination codon regulates both nonstructural polyprotein processing and viral RNA synthesis. Li and Rice replaced the opal termination codon of Sindbis virus with different sense codons and found increased levels of the nsP3/4 polyprotein precursor and reduced levels of mature nsP3 early during infection (18). This study also demonstrated that replacing the opal termination codon with a sense codon led to reduced levels of both 49S genomic and 26S subgenomic viral RNA synthesis early during infection (18). Based on these studies, it will be important to determine whether the Cys codon in AR86 affects neurovirulence through alterations of nonstructural polyprotein processing and/or viral RNA synthesis, which may exert subtle effects on viral replication or affect a yet to-be-defined interaction with the host.

The neurovirulence determinant within the E2 glycoprotein at position 243, where AR86 encodes a unique serine residue, most likely affects early viral interactions with neurons or other cell types in the infected animal. This change is near a region of E2 that is associated with receptor attachment, which raises the strong possibility that the Ser residue might affect virus-receptor interactions either through direct receptor interactions or by changing the conformation of the E2 glycoprotein (24). This is supported by findings within the E2 glycoprotein of Sindbis virus, in that a Gly residue at position 172 enhanced viral binding to neuronal cells (29). Therefore, additional studies to evaluate the effect of Ser versus Leu at E2 position 243 on virus binding or infection of neurons may provide useful information on the role of this determinant in regulating viral infection of neurons or other cell types. However, the lack of a clearly defined neuronal receptor for alphaviruses currently prevents a direct analysis of this determinant's role in virus-receptor interactions.

In conclusion, we have identified major determinants of Sindbis virus adult mouse neurovirulence by using two closely related neurovirulent and nonneurovirulent Sindbis-group viruses. These determinants are nsP1 position 538, a deletion in nsP3 between 386 and 403, nsP3 position 537, and E2 position 243. Further studies to determine whether these virulence determinants act by affecting viral RNA synthesis or cell tropism or through some as yet undefined interaction with the infected host are under way.

REFERENCES

1. de Groot, R. J., T. Rumenapf, R. J. Kuhn, E. G. Strauss, and J. H. Strauss. 1991. Sindbis virus RNA polymerase is degraded by the N-end rule pathway. Proc. Natl. Acad. Sci. USA 88:8967–8971.
2. Dropulic, L. K., J. M. Hardwick, and D. E. Griffin. 1997. A single amino acid change in the E2 glycoprotein of Sindbis virus confers neurovirulence by altering an early step of virus replication. J. Virol. 71:6100–6105.
3. Dubuisson, J., S. Lustig, N. Ruggli, Y. Akov, and C. M. Rice. 1997. Genetic determinants of Sindbis virus neuroinvasiveness. J. Virol. 71:2636–2646.
4. Griffin, D. E. 2001. Alphaviruses, p. 917–962. In D. M. Knipe, B. N. Fields, and P. M. Howley (ed.), Fields virology, 4th ed. Lippincott Williams & Wilkins, Philadelphia, Pa.
5. Griffin, D. E. 1989. Molecular pathogenesis of Sindbis virus encephalitis in experimental animals. Adv. Virus Res. 36:255–271.
6. Griffin, D. E. 1976. Role of the immune response in age-dependent resistance of mice to encephalitis due to Sindbis virus. J. Infect. Dis. 133:456–464.
7. Griffin, D. E., and R. T. Johnson. 1977. Role of the immune response in recovery from Sindbis virus encephalitis in mice. J. Immunol. 118:1070–1075.
8. Griffin, D. E., B. Levine, W. R. Tyor, P. C. Tucker, and J. M. Hardwick. 1994. Age-dependent susceptibility to fatal encephalitis: alphavirus infection of neurons. Arch. Virol. Suppl. 9:31–39.
9. Heise, M. T., D. A. Simpson, and R. E. Johnston. 2000. A single amino acid change in nsP1 attenuates neurovirulence of the Sindbis-group alphavirus S.A.AR86. J. Virol. 74:4207–4213.
10. Heise, M. T., L. J. White, D. A. Simpson, C. Leonard, K. A. Bernard, R. B. Meeker, and R. E. Johnston. 2003. An attenuating mutation in nsP1 of the Sindbis-group virus S.A.AR86 accelerates nonstructural protein processing and up-regulates viral 26S RNA synthesis. J. Virol. 77:1149–1156.
11. Klimstra, W. B., H. W. Heidner, and R. E. Johnston. 1999. The furin protease cleavage recognition sequence of Sindbis virus PE2 can mediate virion attachment to cell surface heparan sulfate. J. Virol. 73:6299–6306.
12. Kobiler, D., C. M. Rice, C. Brodie, A. Shahar, J. Dubuisson, M. Halevy, and S. Lustig. 1999. A single nucleotide change in the 5′ noncoding region of Sindbis virus confers neurovirulence in rats. J. Virol. 73:10440–10446.
13. Labrada, L., X. H. Liang, W. Zheng, C. Johnston, and B. Levine. 2002. Age-dependent resistance to lethal alphavirus encephalitis in mice: analysis of gene expression in the central nervous system and identification of a novel interferon-inducible protective gene, mouse ISG12. J. Virol. 76:11688–11703.
14. Lastarza, M. W., A. Grakoui, and C. M. Rice. 1994. Deletion and duplication mutations in the C-terminal nonconserved region of Sindbis virus nsP3: effects on phosphorylation and on virus replication in vertebrate and invertebrate cells. Virology 202:224–232.
15. Levine, B., J. E. Goldman, H. H. Jiang, D. E. Griffin, and J. M. Hardwick. 1996. Bcl-2 protects mice against fatal alphavirus encephalitis. Proc. Natl. Acad. Sci. USA 93:4810–4815.
16. Levine, B., Q. Huang, J. T. Isaacs, J. C. Reed, D. E. Griffin, and J. M. Hardwick. 1993. Conversion of lytic to persistent alphavirus infection by the bcl-2 cellular oncogene. Nature 361:739–742.
17. Li, G. P., M. W. La Starza, W. R. Hardy, J. H. Strauss, and C. M. Rice. 1990. Phosphorylation of Sindbis virus nsP3 in vivo and in vitro. Virology 179:416–427.
18. Li, G. P., and C. M. Rice. 1989. Mutagenesis of the in-frame opal termination codon preceding nsP4 of Sindbis virus: studies of translational readthrough and its effect on virus replication. J. Virol. 63:1326–1337.
19. Lustig, S., A. C. Jackson, C. S. Hahn, D. E. Griffin, E. G. Strauss, and J. H. Strauss. 1988. Molecular basis of Sindbis virus neurovirulence in mice. J. Virol. 62:2329–2336.
20. Malherbe, H., M. Strickland-Cholmley, and A. L. Jackson. 1963. Sindbis virus infection in man. Report of a case with recovery of virus from skin lesions. S. Afr. Med. J. 37:547–552.
21. Sambrook, J., E. Fritsch, and T. Maniatis. 1989. Molecular cloning: a laboratory manual, 2nd ed. Cold Spring Harbor Laboratory, Cold Spring Harbor, N.Y.
22. Sarkar, G., and S. S. Sommer. 1990. The "megaprimer" method of site-directed mutagenesis. BioTechniques 8:404–407.

23. **Simpson, D. A., N. L. Davis, S. C. Lin, D. Russell, and R. E. Johnston.** 1996. Complete nucleotide sequence and full-length cDNA clone of S.A.AR86 a South African alphavirus related to Sindbis. Virology **222:**464–469.

24. **Smith, T. J., R. H. Cheng, N. H. Olson, P. Peterson, E. Chase, R. J. Kuhn, and T. S. Baker.** 1995. Putative receptor binding sites on alphaviruses as visualized by cryoelectron microscopy. Proc. Natl. Acad. Sci. USA **92:**10648–10652.

25. **Strauss, J. H., and E. G. Strauss.** 1994. The alphaviruses: gene expression, replication, and evolution. Microbiol. Rev. **58:**491–562.

26. **Trgovcich, J., J. F. Aronson, J. C. Eldridge, and R. E. Johnston.** 1999. TNFalpha, interferon, and stress response induction as a function of age-related susceptibility to fatal Sindbis virus infection of mice. Virology **263:**339–348.

27. **Trgovcich, J., J. F. Aronson, and R. E. Johnston.** 1996. Fatal Sindbis virus infection of neonatal mice in the absence of encephalitis. Virology **224:**73–83.

28. **Trgovcich, J., K. Ryman, P. Extrom, J. C. Eldridge, J. F. Aronson, and R. E. Johnston.** 1997. Sindbis virus infection of neonatal mice results in a severe stress response. Virology **227:**234–238.

29. **Tucker, P. C., and D. E. Griffin.** 1991. Mechanism of altered Sindbis virus neurovirulence associated with a single-amino-acid change in the E2 glycoprotein. J. Virol. **65:**1551–1557.

30. **Tucker, P. C., S. H. Lee, N. Bui, D. Martinie, and D. E. Griffin.** 1997. Amino acid changes in the Sindbis virus E2 glycoprotein that increase neurovirulence improve entry into neuroblastoma cells. J. Virol. **71:**6106–6112.

31. **Tucker, P. C., E. G. Strauss, R. J. Kuhn, J. H. Strauss, and D. E. Griffin.** 1993. Viral determinants of age-dependent virulence of Sindbis virus for mice. J. Virol. **67:**4605–4610.

32. **Tuittila, M., and A. E. Hinkkanen.** 2003. Amino acid mutations in the replicase protein nsP3 of Semliki Forest virus cumulatively affect neurovirulence. J. Gen. Virol. **84:**1525–1533.

33. **Tuittila, M. T., M. G. Santagati, M. Roytta, J. A. Maatta, and A. E. Hinkkanen.** 2000. Replicase complex genes of Semliki Forest virus confer lethal neurovirulence. J. Virol. **74:**4579–4589.

34. **Weinbren, M. P., R. H. Kokernot, and K. C. Smithburn.** 1956. Strains of Sindbis-like virus isolated from culicine mosquitoes in the Union of South Africa. I. Isolation and properties. S. Afr. Med. J. **30:**631–636.